JOURNAL OF MATERIALS SCIENCE 30 (1995) 3274–3278

Preparation of spherical $Zr_{0.8}Sn_{0.2}TiO_4$ powder by ultrasonic spray pyrolysis

SEO-YONG CHO, JONG-HEUN LEE, SOON JA PARK
Department of Inorganic Materials Engineering, Seoul National University, Kwanak-Ku, Seoul, 151-742, Korea

Fine, spherical $Zr_{0.8}Sn_{0.2}TiO_4$ powders were prepared by spray pyrolysis, using an ultrasonic transducer, from an aqueous solution of metal chlorides. The synthesized powders had a spherical morphology and many shell fragments. The observed shell fragments were attributed to the impermeable surface crust formed during thermal decomposition of the droplets. The raw materials for the preparation of $Zr_{0.8}Sn_{0.2}TiO_4$ were analysed prior to any treatments because the properties of the surface crust could be related to those of the raw materials. $ZrOCl_2 \cdot 8H_2O$ was supposed to affect the shell fragments as well. Spherical $Zr_{0.8}Sn_{0.2}TiO_4$ powders without shell fragments could be prepared using $ZrO(CH_3COO)_2$ in place of $ZrOCl_2 \cdot 8H_2O$.

1. Introduction

In recent years, the demand for ceramic dielectric materials has been increased and many kinds of dielectric materials including $(Zr,Sn)TiO_4$ $Ba(Zn,Ta)O_3$–$Ba(Zn,Nb)O_3$, BaO–PbO–Nd_2O_3–TiO_2 and $MgTiO_3$–$CaTiO_3$ have been developed for microwave applications [1]. Zirconium titanate solid solutions, $Zr_xSn_yTi_zO_4 (x + y + z = 2)$, are of interest due to the superior dielectric properties – high dielectric constant, high Q value and low temperature coefficient of resonant frequency – in the microwave frequency regime.

Many researchers have studied the $Zr_xSn_yTi_zO_4$ system [2–6], hereinafter referred to as ZST, and most of them prepared the ZST powders using a solid-state reaction, i.e., the mixture of ZrO_2, SnO_2, and TiO_2 was calcined at about 1100 °C. The solid-state reactions take place at high temperatures by the mutual diffusion of cations through oxygen lattices by way of the contact areas between the particles of different oxides. The decrement of the active surface of the powder usually occurs because the solid-state reaction is accompanied by sintering [7]. Therefore, it has been difficult to get a high-density ZST using the powders from the solid-state reaction. This required the use of sintering additives such as ZnO, NiO, CdO, La_2O_3 etc. [2–5]. These additives, however, have been reported to cause the degradation of the dielectric properties of pure ZST [6]. In addition, the composition of ZST powders from the solid-state reaction is usually found to be inhomogeneous. It is known that the preparation of homogeneous ZST powders with high sinterability is a prerequisite to achieving better dielectric properties.

Spray pyrolysis is one of the promising methods which can prepare spherical powders with reproducibility. It also controls the particle size easily by varying the concentration of the precursor solution or atomization parameters [8]. In spray pyrolysis, a salt solution is atomized into a heated reaction chamber where the droplets dry to form the precursor salts and then it decomposes directly to form the oxide. The compositional heterogeneity of the powders exists only within one spherical, secondary particle because each droplet acts as a seperate reactor in the decomposition reaction [9]. Many kinds of superconductor with relatively complex compositions have been prepared by spray pyrolysis because of its aforementioned easiness in the control of micro-compositional heterogeneity [10–12]. Therefore, the preparation of ZST powders by spray pyrolysis is regarded as superior to that by the solid-state reaction in view of the morphology and compositional homogeneity. The preparation of ZST powders, however, by spray pyrolysis has never been reported.

In this study, spherical ZST powders were prepared by ultrasonic spray pyrolysis from (1) the aqueous solution of $ZrOCl_2 \cdot 8H_2O$, $SnCl_4 \cdot xH_2O$ and $TiCl_4$ and (2) that of $ZrO(CH_3COO)_2$, $SnCl_4 \cdot xH_2O$ and $TiCl_4$. The factors affecting the morphology, size and phase of the powders have been studied.

2. Experimental procedure

Metal chlorides were used as source materials because they are economical and highly soluble in water. Aqueous precursor solutions were made up using appropriate weights of (1) $TiCl_4$ (GR grade) $SnCl_4 \cdot xH_2O$ (GR grade) $ZrOCl_2 \cdot 8H_2O$ (GR grade) and (2) $TiCl_4$ $SnCl_4 \cdot xH_2O$, $ZrO(CH_3COO)_2$ (> 98%) in distilled water with the atomic ratio of Zr:Sn:Ti of 0.8:0.2:1.

The solution concentrations ($= [Ti^{+4}] = [Zr^{+4}] + [Sn^{+4}]$ were varied from 0.2 M to 0.004 M.

0022–2461

The precursor solutions were sprayed by an ultrasonic transducer (resonant frequency = 1.67 MHz) and the droplets passed into a quartz tube (inner diameter = 30 mm) heated at various temperatures with a carrier gas. N_2 was used as a carrier gas and the flow rate was 0.8 l min^{-1}. The synthesized powders were collected in distilled water and dried in an oven. A schematic diagram of the experimental apparatus is shown elsewhere [13].

3. Results and discussion

Fig. 1 shows the X-ray diffraction (XRD) patterns of the ZST powders prepared at 500, 700 and 900 °C from 0.2 M precursor solution. The powders prepared above 700 °C show the ZST single phase, while the unidentified and amorphous phases were found in the powder at 500 °C. The ZST and other unidentified phases were mixed at 600 °C although this is not shown in this paper. It indicates that the ZST single phase can be obtained about 600–700 °C in this experiment, which is a much lower temperature than that of the solid-state reaction. The reduction in the temperature for the preparation of the ZST phase without any minor component might result from the submicro-scale reaction due to the homogeneous distribution of the cations in a droplet.

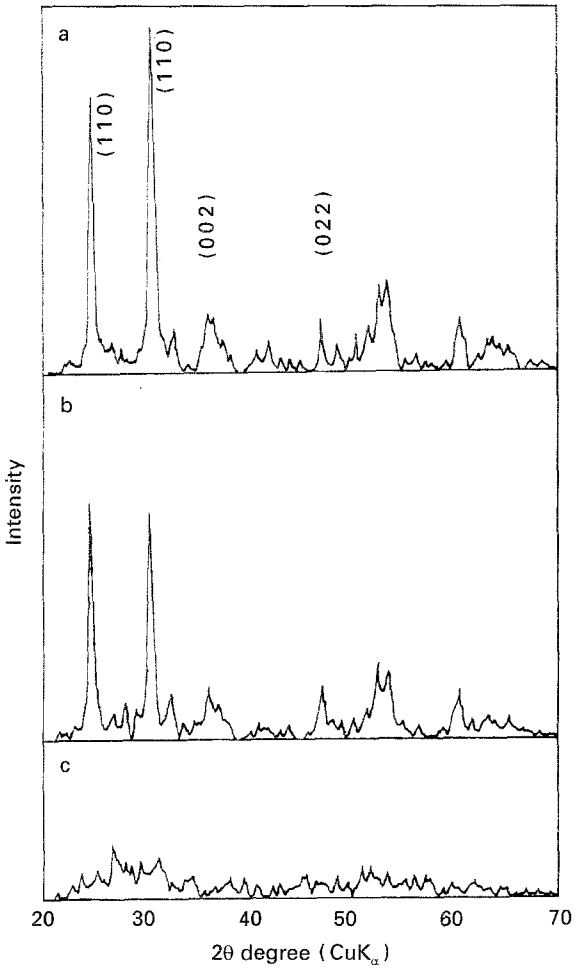

Figure 1 X-ray diffraction patterns of the ZST powders prepared from 0.2 M solution at various temperatures; (a) 900 °C; (b) 700 °C; (c) 500 °C.

To study the decomposition characteristics of the precursor solutions, the solutions were dried at 100 °C for 1 day and evaluated by thermogravimetric analysis (TGA) and differential thermal analysis (DTA) with a heating rate of 10 °C min^{-1} in a N_2 atmosphere (Fig. 2). The TGA curve in Fig. 2 shows that the decomposition of the precursors finished at about 600 °C and little weight loss was observed above 600 °C. The endothermic peaks at 184 °C in the DTA curve was due to the dehydration of the precursors. Two exothermic peaks located at 514 °C and 581 °C were related to the decomposition of the intermediates and the crystallization of the ZST phase, respectively. This crystallization point is lower than that from the XRD study. The difference in crystallization temperatures between XRD and DTA studies could originate from the kinetic effects. Since, in spray pyrolysis, the droplets passed through the hot zone for only a short period (10–15 s in this experiment), the heating rate must be very high. Accordingly, the droplet could not receive enough heat and the decomposition reaction was fully completed at a higher temperature than that of the DTA curve. It is natural to have a higher temperature than 600 °C to produce ZST single phase by spray pyrolysis.

Fig. 3 shows scanning electron microscopy (SEM) micrographs (Jeol, JEM 200-CX, Japan) of the ZST powders prepared at 800 °C from various concentrations of the solution. All powders exhibited a spherical shape and sizes in the range of 0.1 to 2.0 μm. The arithmetic mean diameters of particles were 0.94 ± 0.47 μm for 0.1M, 0.53 ± 0.27 μm for 0.04 M, and 0.19 ± 0.11 μm for 0.004 M, respectively. The particle sizes were obtained from the direct measurement of particles in transmission electron microscopy (TEM) micrographs (Jeol, JSM-840A, Japan) and more than 500 particles were measured in each concentration. The particles show the dependency on the concentration of the precursor solution, that is, the size of particles decreased with the concentration of the solution. The relationship between particle size and solution concentration has already been discussed [14–16] and in any case, the size of the particles decreases as concentration of the solution decreases.

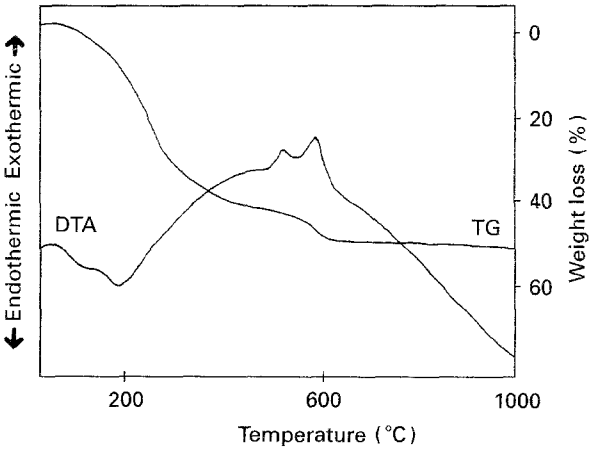

Figure 2 DTA/TGA curves of the precursor solution in N_2 at a heating rate of 10 °C min^{-1}.

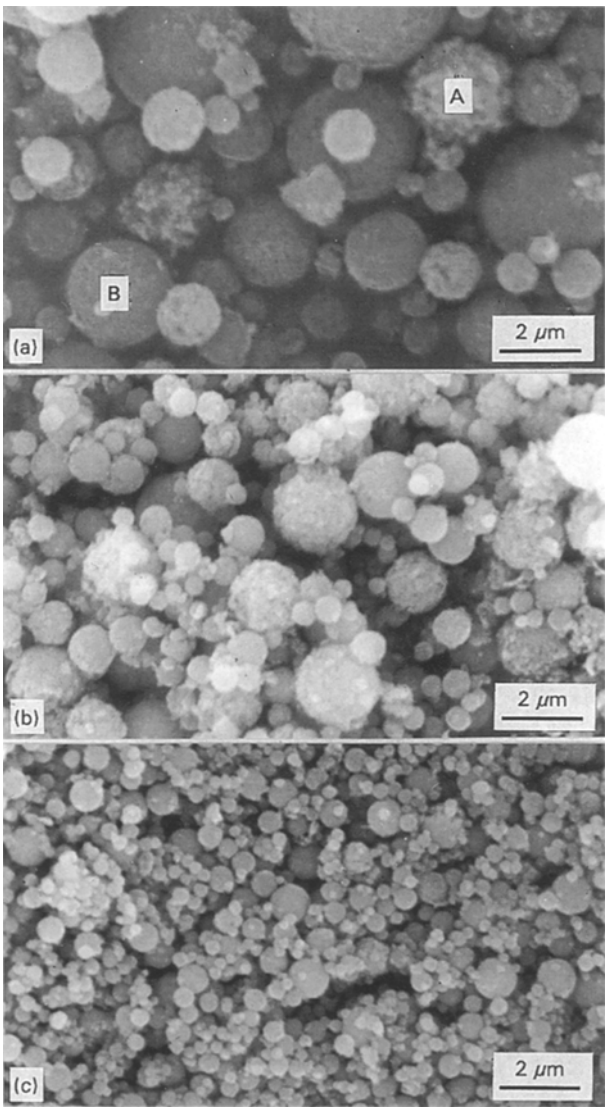

Figure 3 SEM micrographs of the ZST powders prepared at 800 °C from various solution concentrations; (a) 0.1 M; (b) 0.04 M; (c) 0.004 M.

The particle-size distributions for powders shown in Fig. 3 are presented in Fig. 4. The abscissa represents for the particle size which was normalized by the arithmetic mean diameter at each concentration and the ordinate, frequency. It shows a narrow size distribution and the distribution did not change even if the concentration of the precursor solution was varied. This means that the formation mechanisms of the three kinds of powders were identical [13].

It can be seen that the particles in Fig. 3 have many shell fragments. Many factors such as reaction temperature, gas flow rate, and source materials etc., have effects on the powder morphology. It is generally acknowledged that the physical characteristics of the dried salts which were related to source materials had the largest effect on the morphology of the resultant oxide powders. In spray pyrolysis, the sprayed droplets were moved into high temperature reactors and the water solvent started evaporation from the outer part of the droplet. This resulted in the localized supersaturation of the solute and the salt precipitated at the droplet surface. A salt crust was formed before the droplet was completely dried when the evaporation proceeded faster than the counterdiffusion of the solute from the surface to the inner part of the droplet. If the crust layer is hard and impermeable to gas, the vapour/gas from the inner part of the droplet can not exit and fracture of the crust occurs. If the crust layer is hard and permeable, the vapour can diffuse through the layer and fragments of the prepared powders seemed to be caused by impermeable crusts formed during the decomposition process.

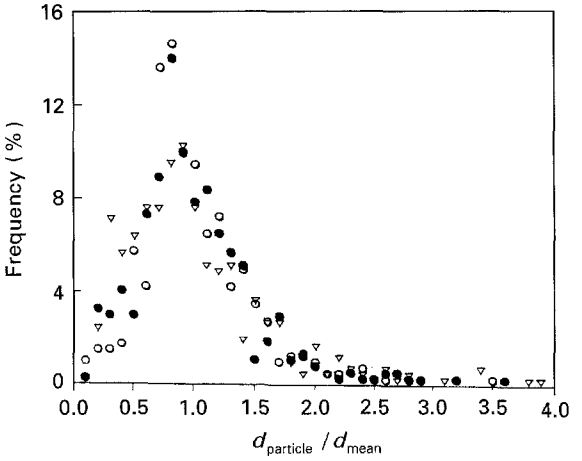

Figure 4 Size distribution of the ZST powders prepared at 800 °C from various concentrations. ○ 0.1 M; ● 0.04 M; ▽ 0.004 M.

Charlesworth and Marshall [17] have suggested that the outer surface was usually smooth and the inner surface was rough and uneven when the surface crust was formed. Considering these facts, the lumpy surface of the powder (see A in Fig. 3(a)) seemed to be the fractured inner surface and smooth surface (see B in Fig. 3(a)) seemed to be the unfractured outer surface. Consequently, the factor which caused shell fragments was the impermeable surface crusts and the raw materials which form the impermeable crust should be revealed to improve the powder morphology.

ZrO_2 powder was prepared by spray pyrolysis from $ZrOCl_2 \cdot 8H_2O$, TiO_2 from TiC_4, SnO_2 from $SnCl_4 \cdot xH_2O$, respectively, in the same conditions used as in the preparation of the ZST powders. This is to reveal the raw materials which largely affected the shell fragments. As seen in Fig. 5, SnO_2 powders had a smooth surface and no fragments, while TlO_2 had a smooth surface with a few fragments. On the other hand, ZrO_2 powders had a lumpy surface and many shell fragments. Compared to the ZST powders in Fig. 4, the morphology of the ZrO_2 powders was similar to that of ZST powders. Zhang and Messing [18] have prepared ZrO_2 powders by the same process using several zirconium-source materials and reported similar results to those obtained with $ZrOCl_2 \cdot 8H_2O$.

Therefore, $ZrOCl_2 \cdot 8H_2O$ is assumed to affect the shell fragments of the ZST powders. However, the influence of $TiCl_4$ and the mutual interaction between raw materials should be considered as well. The $Zr_{0.2}Sn_{0.8}TiO_4$ powders were prepared from $ZrOCl_2 \cdot 8H_2O$, $SnCl_4$ and $TiCl_4$ and compared to $Zr_{0.8}Sn_{0.2}TiO_4$ powders to confirm the above influences. As seen in Fig. 6 the $Zr_{0.2}Sn_{0.8}TiO_4$ powders which had a relatively small ZrO_2 concentration (i.e.

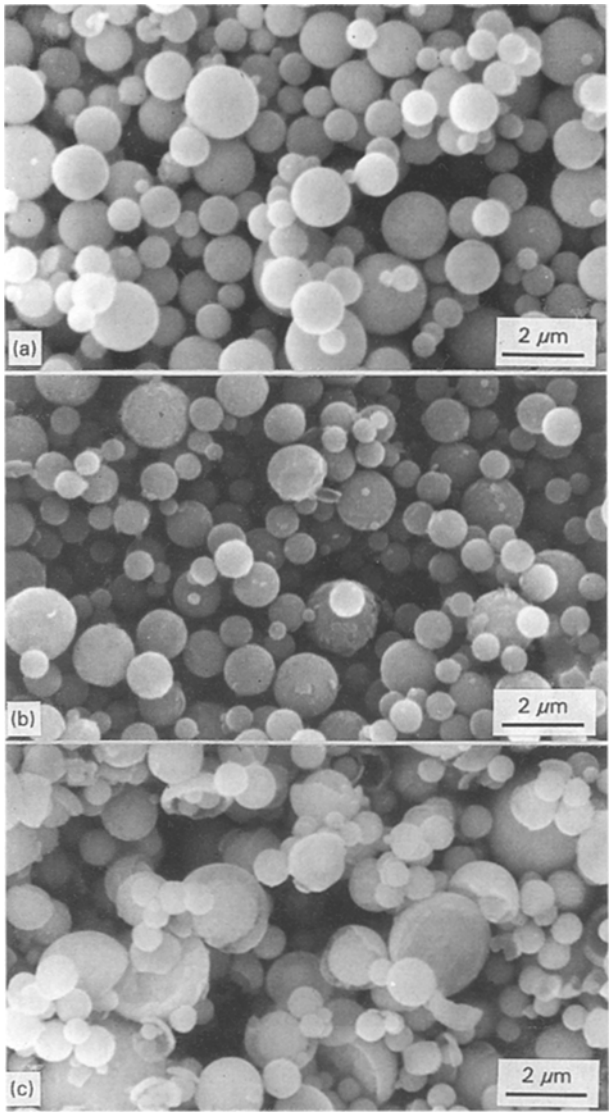

Figure 5 SEM micrographs of the SnO_2 TiO_2 and ZrO_2 powders prepared at 800 °C from 0.2 M solution; (a) SnO_2; (b) TiO_2; (c) ZrO_2.

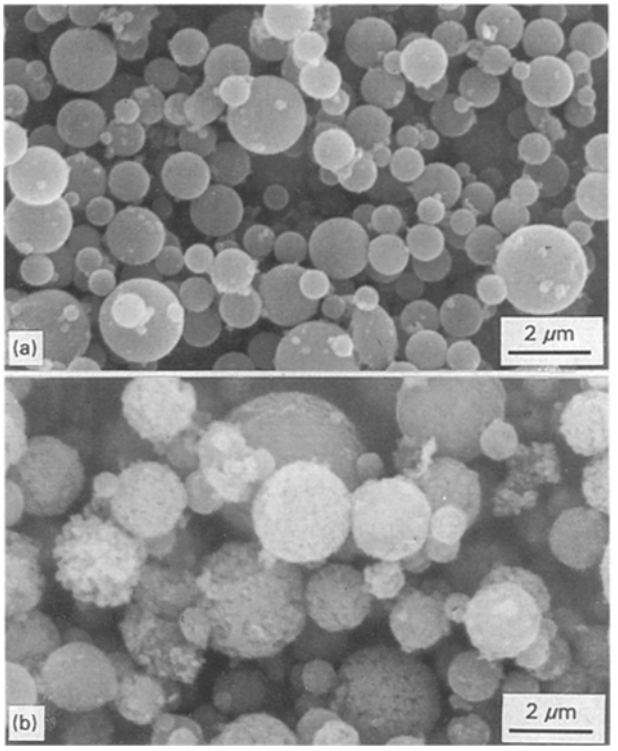

Figure 6 SEM micrographs of the $Zr_{0.2}Sn_{0.8}TiO_4$ and $Zr_{0.8}Sn_{0.2}TiO_4$ powders prepared at 800 °C from 0.1 M solution; (a) $Zr_{0.2}Sn_{0.8}TiO_4$; (b) $Zr_{0.8}Sn_{0.2}TiO_4$.

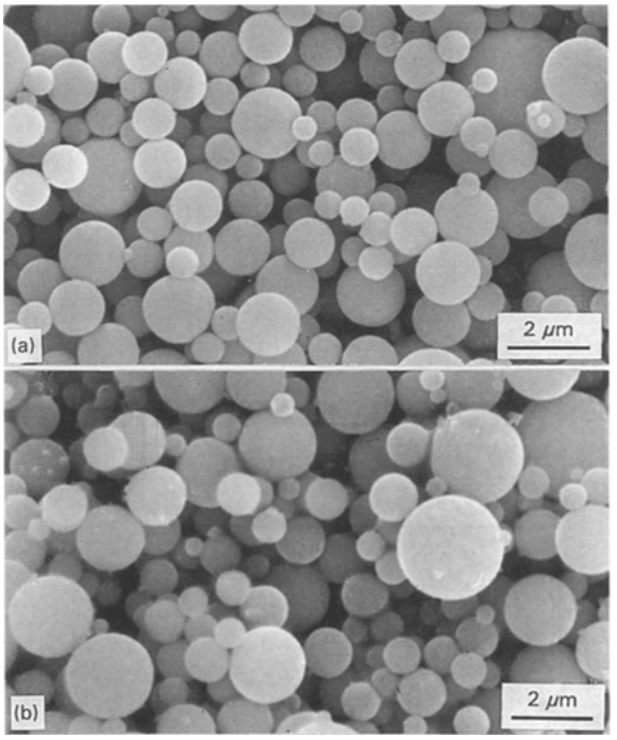

Figure 7 SEM micrographs of the ZrO_2 and ZST powders prepared at 800 °C from 0.1 M solution using ZrO $(CH_3COO)_2$; (a) ZrO_2 (b) ZST.

small $ZrOCl_2 \cdot 8H_2O$ content) and the same $TiCl_4$ concentration had a smooth surface and no fragments, which indicated that the shell fragments of the prepared ZST powders were strongly dependent on the amount of $ZrOCl_2 \cdot 8H_2O$. Consequently, it might be said that $ZrOCl_2 \cdot 8H_2O$ affects the morphology of the prepared ZST powders and other zirconium source materials were required to improve the powder morphology.

Several zirconium-source materials were used in the ZrO_2 powder preparation for preliminary experiments and the powders obtained from $ZrO(CH_3COO)_2$ had a good morphology without shell fragments. The $ZrO(CH_3COO)_2$ was selected in place of $ZrOCl_2 \cdot 8H_2O$ and ZST powders from $ZrO(CH_3COO)_2$ were prepared in the same condition as in the case of $ZrOCl_2 \cdot 8H_2O$. Fig. 7 shows SEM micrographs of the ZrO_2 powders from $ZrO(CH_3COO)_2$ and the ZST powders from $ZrO(CH_3COO)_2TiCl_4$ and $SnCl_4 \cdot xH_2O$. As shown in the figure, the ZrO_2 and ZST powders using $ZrO(CH_3COO)_2$ had a spherical morphology and no fragments. This also supports the above explanation that the shell fragments of the prepared ZST powders were due to $ZrOCl_2 \cdot 8H_2O$.

Sproson *et al.* [19] have reported that the acetate-driven powders prepared by spray pyrolysis showed different morphologies from the nitrate-driven powders in case of NiO, MgO and ZnO. They suggested

that the difference is attributed to the exothermic oxidation which occurred during the decomposition of the acetate salts in air. In a N_2 atmosphere, the exothermic oxidation of acetate salts did not occur and the powders from the acetate had a similar morphology to those from the nitrate. However, the different morphology between acetate-driven and chloride-driven ZST powders in these experiments might not be due to the exothermic oxidation because the powders were prepared in N_2. The difference could be due to the permeable crust formed from $ZrO(CH_3COO)_2$ although further studies are required to reveal the exact role of $ZrO(CH_3COO)_2$.

4. Conclusions

Spherical, fine $Zr_{0.8}Sn_{0.2}TiO_4$ powders were prepared by spray pyrolysis using an aqueous solution of $ZrOCl_2 \cdot 8H_2O/ZrO(CH_3COO)_2$, $SnCl_4 \cdot xH_2O$ and $TiCl_4$. The ZST powders without any minor phase could be prepared above 700 °C and particle size ranged from 0.1 to 2 μm. The powders obtained from chlorides show a spherical morphology with many shell fragments. These shell fragments might be due to the low permeability of the surface crust. The salt characteristics of $ZrOCl_2 \cdot 8H_2O$ were considered to affect the shell fragments. The spherical ZST powders without shell fragments could be prepared using $ZrO(CH_3COO)_2$ in place of $ZrOCl_2 \cdot 8H_2O$.

Acknowledgements

We wish to express our gratitude to Professor M. C. Kim in Kunsan National University for facilitating DTA/TGA experiments in his laboratory and Professor S. H. Kang in Seoul National University for a critical reading of the manuscript. Funding for this work is provided by Highly Advanced National Project. The support of Ministry of Science and Technology is gratefully acknowledged. We express our gratitude to Professor S. H. Kang in Seoul National University for a critical reading of the manuscript.

References

1. K. WAKINO, T. NISHIKAWA, Y. ISHIKAWA and H. TAMURA, *Br. Ceram. Trans. J.* **89** (1990) 39.
2. G. WOLFRAM and H. E. GOBEL, *Mater. Res. Bull.* **16** (1981) 1455.
3. Y. C. HEIAO, L. WU and C. C. WEI, *ibid.* **23** (1988) 1687.
4. K. WAKINO, K. MINAI and H. TAMURA, *J. Amer. Ceram. Soc.* **67** (1984) 278.
5. F. AZOUGH and R. FREER, *Br. Ceram. Proc.* **37** (1986) 225.
6. S. HIRANO, T. HAYASHI and A. HATTORI, *J. Amer. Ceram. Soc.* **74** (1991) 1320.
7. J. G. DELAU, *Amer. Ceram. Soc. Bull.* **49** (1970) 572.
8. S. C. ZHANG and G. L. MESSING, in "Ceramic transactions", Vol. 12, "Ceramic Powder Science III", edited by G. L. Messing, S. Hirano and H. Hausner (American Ceramic Society, Westerville, OH, 1990) p. 49.
9. J. H. LEE and S. J. PARK, *J. Mater. Sci.; Materials in Electronics* (in press).
10. Y. KANNO and K. NAKANO, *J. Mater. Sci. Lett.* **9** (1990) 1229.
11. I. T. KIM, T. S. OH and Y. H. KIM, *J. Mater. Sci.* **26** (1991) 6275.
12. T. L. WARD, T. T. KODAS and A. H. CARIM, *J. Mater. Res.* **7** (1992) 827.
13. J. H. LEE, H. J. CHO and S. J. PARK in "Ceramic Transactions", Vol. 22, "Ceramic Powder Science IV", edited by S. Hirano, G. L. Messing and H. Hausner (American Ceramic Society, Westerville, OH, 1991) p. 39.
14. D. M. ROY, R. R. NEURGAONKAR, T. P. O'HOLLERN and R. ROY, *Amer. Ceram. Soc. Bull.* **56** (1977) 1023.
15. K. NONAKA, T. YANO and N. OTSUKA, *J. Ceram. Soc. Jpn Inter. Ed.* **97** (1989) 928.
16. J. H. LEE and S. J. PARK, *J. Amer. Ceram. Soc.* **76** (1993) 777.
17. D. H. CHARLESWORTH and W. R. MARSHALL Jr, *A.I.Ch.E. Journal* **6** (1960) 9.
18. S. C. ZHANG, G. L. MESSING and M. BORDEN, *J. Amer. Ceram. Soc.* **73** (1990) 61.
19. D. W. SPROSON, G. L. MESSING and T. J. GARDNER, *Ceramics International* **12** (1986) 3.

Received 22 October 1993
and accepted 9 January 1995